

### Tunnelling effect on the adjacent pile footings

Mona M.Eid<sup>1</sup>, Ali A. A. Ahmed<sup>1</sup>, Ashraf M. Hefny<sup>2</sup> and Ahmed N.EL-Attar<sup>3</sup>

<sup>1</sup>Professor of Geotechnical Engineering, Structure Engineering Department, Ain Shams University

<sup>2</sup>Associate Professor of Geotechnical Engineering, Structure Engineering Department, Ain Shams University/UAE.U

<sup>3</sup>Assistant Lecturer, Civil Engineering Department, Higher Technology institute.

[Ahmed\\_civil\\_hti@yahoo.com](mailto:Ahmed_civil_hti@yahoo.com)

**Abstract:** Tunnelling activities in urban areas are always associated with surface and subsurface ground subsidence, which may affect the stability of nearby structures and utilities. In cases, where these structures founded utilizing deep foundation systems, the ground subsidence associated with tunnelling must be cautiously considered because in most cases of shallow tunnelling conditions, the deep foundations may be located in the zones of influence of tunnelling activities. Also, the characteristics of ground-pile interaction play an important role in the stability of these structures. The main objective of the present study is to numerically evaluate the nature of interaction between the employed tunnelling technology and the nearby structures founded on deep foundation systems using 3D finite element idealization. Two case studies of tunnelling projects are employed in the analysis to evaluate the interaction between tunnelling process, confining ground, and the deep foundations arrangement. The first case considers of the stability of El-Attabe Garage building due to the execution of the Greater Cairo Metro Line 3-Phase 1, while the second case considers the stability of an existing motorway constructed of contiguous pile walls due to the construction Metro project crosses below the underpass. In this study, 3D finite element modelling is used to evaluate the tunnelling-ground-pile interaction behaviour due to the different tunnelling activities. The details of the tunnelling process; such as face pressure, rate of shield advancement, lining erection, tail grouting, and the grout hardening are idealized in numerical modelling. Also, the encountered ground stratigraphy with respect to its strength parameters and engineering properties of the deep foundation systems are introduced in the details of numerical modelling. Soil convergence around the tunnel excavation is modelled using a non-associated Mohr-Coulomb failure criterion. Results of the verification of the case histories show a fairly good agreement between measured and the computed data which validate the finite element model.

[Mona M. Eid, Ali A. A. Ahmed, Ashraf M. Hefny and Ahmed N. EL-Attar. **Tunnelling effect on the adjacent pile footings.** *J Am Sci* 2015;11(1):88-98]. (ISSN: 1545-1003). <http://www.jofamericanscience.org>. 12

**Keywords:** Tunnelling, lining, piles, three-dimensional modelling, finite element, grouting.

#### 1. Introduction

The rising volume of obstructions being encountered underground left the tunnel alignments are being left with few alternatives but to excavate within close proximity of existing foundations. Extensive research has been carried out in the United Kingdom particularly on the Jubilee Line Extension (Burland *et al.*, 2002) on the effects of tunnelling on nearby structures. However, most of the structures in the studies are supported on shallow foundations and very little work has been carried out on structures supported on pile foundations. This is due to the fact that most structures were built long before the tunnels are planned. As a result, instrumentation inside existing pile foundation is difficult to install for further investigation.

Early efforts to study tunnel-soil-pile interaction have focused primarily on pile end bearing response and settlement magnitudes, neglecting induced lateral and bending behaviour. However, recent numerical studies by (Loganathan *et al.*, 2001; Mroueh and Shahrour, 2002; Cheng *et al.*, 2004; and Pang *et al.*,

2005) have provided valuable insight and understanding into the various factors that affect the bending performance of piled foundations subjected to tunnelling induced ground movements.

The tunnelling-ground-pile foundation interaction behaviour is typically a 3D problem, in which the details of tunnel advancement crossing the pile foundation system must be idealized in the numerical 3D formulation. 3D finite element idealization is essential to obtain accurate ground subsidence and provide more flexibility in handling complex tunnelling process and soil condition.

In the present study, two case studies of tunnelling-ground-pile systems are idealized and analysed using 3D finite element numerical modelling. The modelling introduces the details of shield tunnelling (face pressure, rate of tunnel advance, lining erection, developed annular gap around excavation, and the tail grouting from soft to hardening condition), ground continuum stratifications and boundary conditions, and the

idealization of the foundation piling system in the global stiffness of the tunnelling-ground-pile system.

## 2. Greater Cairo Metro case history

The implementation of Greater Cairo Metro Line 3 has been started since 2011. The tunnel course extends from Imbaba to Cairo Airport and it will be assembled on four phases with total length 33 km. The tunnel will be executed utilizing a slurry shield Tunnel Boring Machine (TBM) of 9.55 m excavation diameter with tail-skin grouting. The (TBM) length is about 9m with a thickness of a tail piece 5 cm. Face pressure of the bentonite slurry is ranging from 60 to 80 kPa, which provided and controlled by air chamber built into the body of the shield. The tunnel has an internal diameter of 8.35m, external diameter of 9.15m and a precast segmental lining of 0.4m. thickness, Fig.(1). The Greater Cairo Metro, Line 3, Phase-1 runs from El-Attaba Station to El-Abbasia Station and crosses very close to a multi-story car-parking building founded on piles namely, El-Attaba Garage. Fig.(2) shows the locations of the measured vertical surface displacements. There were five surface settlement points installed around the Garage El-Attaba. In this study only two points (S.S.P.b, and S.S.P.c) were considered as they are the nearest points to the investigated building. The building was monitored also during the tunnel advancement from July 2010 to August 2010 at the location of elevation

reference point (ERP.a) (Fig.2). The recorded vertical surface displacements and the building vertical settlements during tunnel advancement were obtained from the National Authority for tunnels (NAT), these settlements were used to allow comparison between the computed 3D modelling deformations and the field measurements complied during tunnel advance.

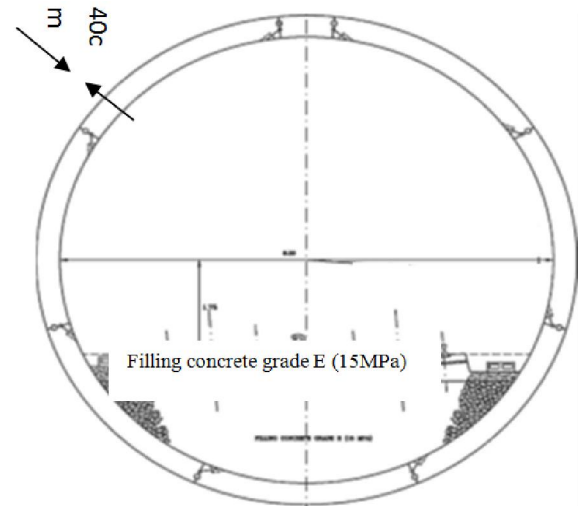


Fig.(1): Cross section profile of Greater Cairo Metro, (after NAT, 2009).

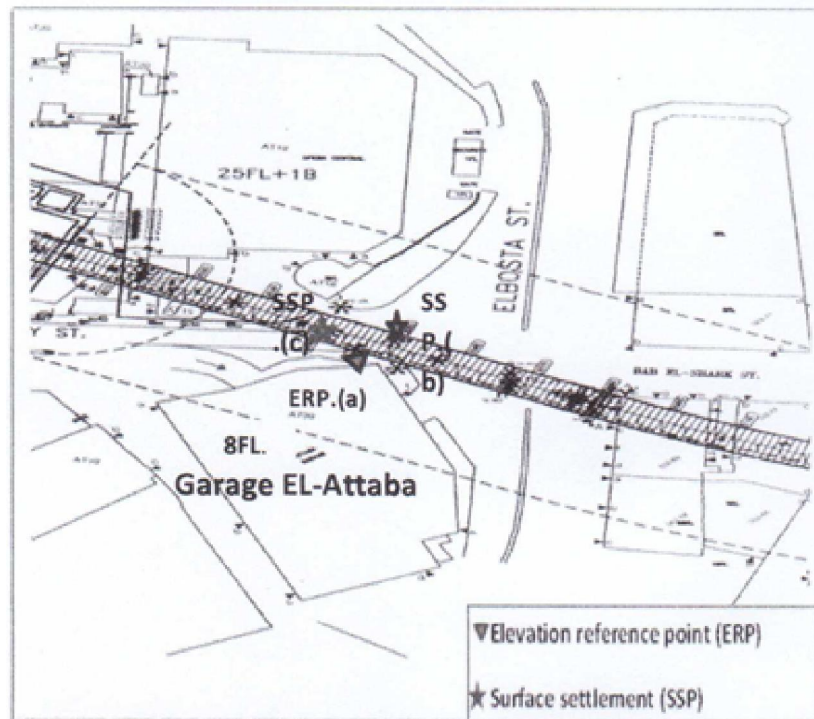


Fig.(2): General layout showing the main settlement points (after Nat., 2010)

## 2.1 Ground conditions

A detailed geotechnical investigation was carried out prior to tunnel construction, which outlined the underlying soil formations beneath the selected building with the various stratigraphic units, (Fig.3). Table (1) summarises the estimated ground geotechnical parameters required for updating the

numerical modelling. The angle of dilation as shown in table (1) depends on the angle of internal friction. For non-cohesive soils (sand, gravel) with the angle of internal friction  $\varphi > 30^\circ$ , the value of dilation angle can be estimated as  $\psi = \varphi - 30^\circ$ . Clays (regardless of over consolidated layers) are characterized by a very low amount of dilation ( $\psi \approx 0$ ).

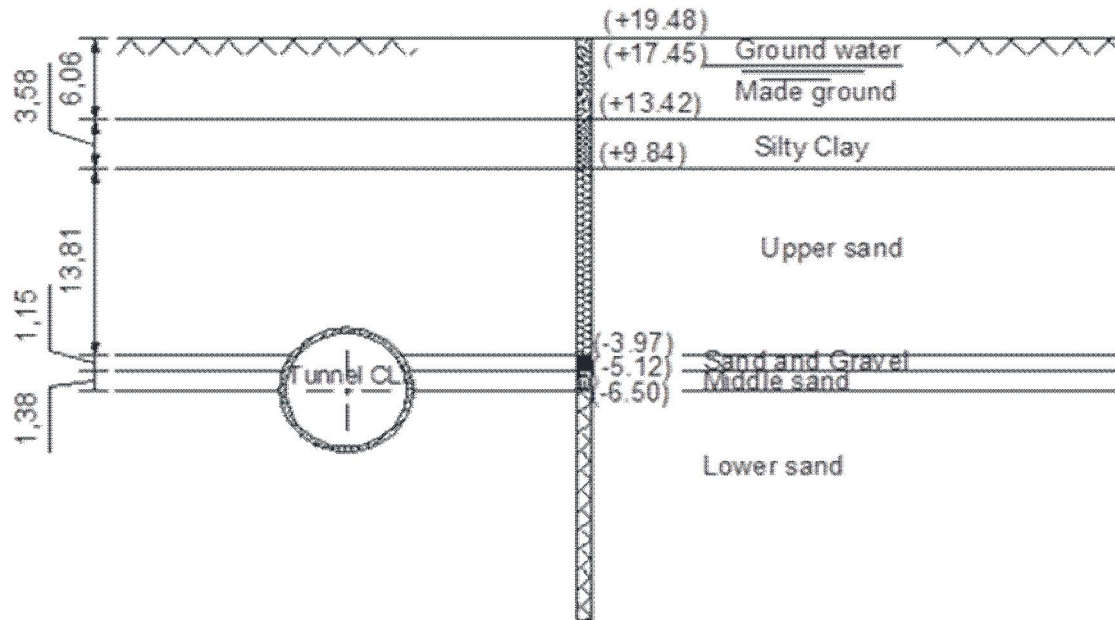


Fig.(3): Subsurface ground conditions underneath Garage EL-Attaba (after Hamza, 2002).

Table (1):The estimated subsurface geotechnical parameters.

Layers	Thick. (m)	$\gamma$ (kN/m <sup>2</sup> )	$\varphi^\circ$	C (kN/m <sup>2</sup> )	E (MN/m <sup>2</sup> )	$\nu$	$\Psi$
Made ground	6.06	17.0	27	0.0	4	0.3	0°
Silty clay	3.58	19.5	$\varphi_d=29^\circ$ $\varphi_u=0^\circ$	$C_d=0.0$ $C_u=90$	$E_d=20$ $E_u=22$	$\nu_d=0.35$ $\nu_u=0.49$	0°
Upper Sand	13.81	19.5	36°	0.0	40	0.3	6°
Sand gravel	1.15	20.0	41°	0.0	100	0.3	11°
Middle sand	1.38	19.5	38	0.0	70	0.3	8°
Lower sand	Extend	19.5	38°	0.0	120	0.3	8°

Note:  $\gamma$ = soil density,  $\phi$ = the internal angle of friction,  $C$ =soil cohesion,  $E$ =Elastic modulus,  $\nu$ = the poisson's ratio,  $\Psi$ =dilation angle

## 2.2 Description of Garage EL-Attaba

El-Attaba car parking is a Skelton type building comprises 8 stories. The building was founded on isolated pile caps supported on 245 bored piles. The piles are 0.6 m in a diameter and extend to 20 m depth to rest in the upper sand layer. The design allowable load carrying capacity for the pile is 120 tons. The building facade is at a horizontal distance of 6.45m from tunnel centreline as shown in Fig. (4). The preliminary analysis indicated that the encircled

pile caps F1, F2, F3, and F4 (figure 4) constitute the critical portion of the building foundation exposed to tunnelling advancement, while the rest of pile caps located outside the zone of influence of tunnelling process. The pile cap (F1) and pile tip location with respect to tunnel axis is shown in Fig.(5). The dimensions of pile caps and arrangement of piles according to consultant (Mocarthy brothers, 1998) are shown in Fig.(6).

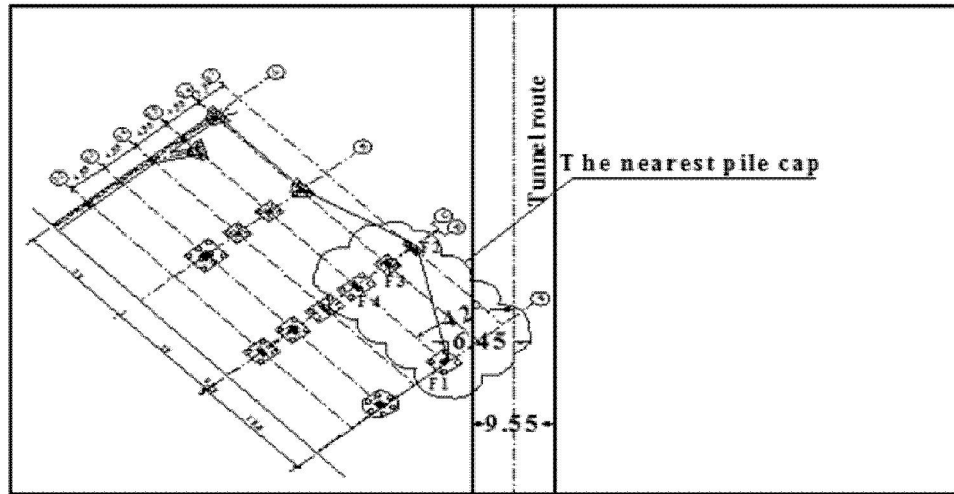


Fig.(4): Location of the nearest pile caps relative to the tunnel route

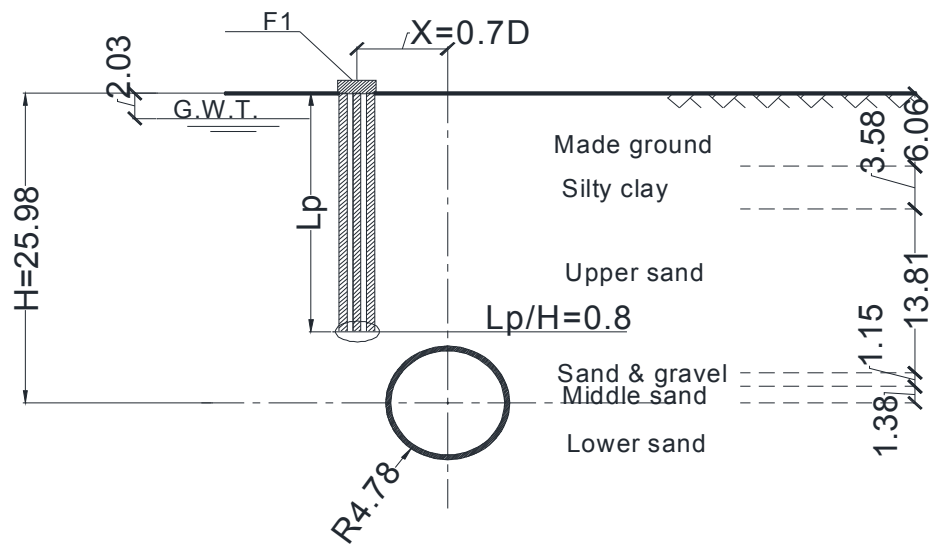


Fig.(5): Location of pile tip relative to tunnel axis level

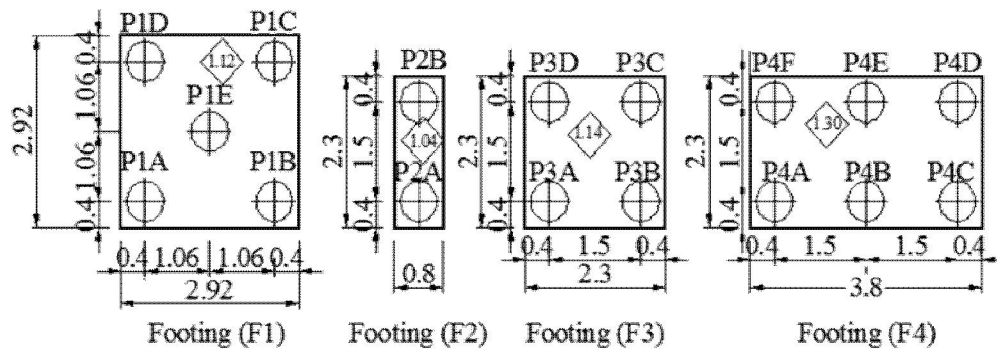


Fig.(6): The dimensions in metres of pile caps and the spacing between piles (after Mocarthy, 1984)

### 2.3 Numerical modelling of Greater Cairo Metrocase study

The 3D modelling of El-Attaba car parking building is formulated using ABAQUS finite element



code, (Hibbitt, Karlsson & Sorensen Inc., 2003). The ground continuum, tunnel lining, piles, and pile caps are modelled using 20-noded continuum solid element. The ground constitutive behaviour is adopted considering the Mohr-coulomb failure criterion. Mohr-Coulomb Model is a first-order model. The model contains five intercept parameters (e.g. Young's modulus,  $E$ , Poisson's ratio,  $\nu$  the effective friction angle,  $\phi'$ , effective cohesion,  $c'$ , and dilatancy angle,  $\psi$ ).

The lining and the shield are assigned to behave as linear elastic material. The elastic properties of the shield elements are assigned to Young's modulus of 200GPa and Poisson's ratio of 0.25, while those of the tunnel lining, pile caps, and piles are updated as 14 GPa and 0.2 respectively. The tail grout used to fill the developed annular ground gap around the TBM due to tunnelling overcutting is updated simultaneously using solid elements. Therefore, calibration with measured surface settlement during shield passage was necessary.

The initial grout element stiffness is assigned to Young's modulus of 1000 kPa and a Poisson's ratio of 0.2 (in the liquid state), while the hardening process is continued with time and the time-dependant Young's modulus is calculated from the grout material compressive strength based on the following empirical relation by Mindess & Young (1981),

$$E(\text{GPa}) = 4.73 \sqrt{f_c} (\text{MPa})$$

Fig. (7) illustrates the 3D numerical model used to simulate the tunnel advancement-ground-piles interaction

#### 2.4 Simulation of tunnel construction

In general, the process of tunnel was modelled in two steps; in the first step, the initial conditions

were set up for the model before excavation of the tunnels. It was achieved by specifying the distribution of effective vertical and horizontal stress (using coefficient of earth pressure at rest). The initial conditions were completed with simulating the four pile caps and its connected piles. In this stage, building loads were calculated and applied to the pile caps. After establishing the initial conditions, the analyses continued with modeling excavation of the tunnel. In the second step, the tunnel advancement was simulated simultaneously considering step-by-step procedure, i.e., implementation of face pressure and starting excavation, lining erection, tail skin grouting, hardening of gout elements from soft to hard state, and finally soil-lining interaction phase. The ground excavation is simulated with 3m length per step. The size of the excavation step changes based on grout mix setting time and the tunnel advancement rate as follows. The grout mix setting time is assigned in the range of 5 to 12 hours, (Shirlaw *et al.*, 2004). Considering, tunnel advancement rate of 9m/day, the corresponding length of grout to be in fluid state would be between 1.875 and 4.5 m. Therefore, the length of initial grout is modelled as 3m length. In the subsequent tunnel advancement, the initial grout element is replaced with grout of hardened property.

The TBM advancement rate of 9m/day is simulated in the analysis. During each excavation step, soil elements are removed with simultaneous application of face pressure on the tunnel face and application of the shield and overcutting grouting elements. At the same step, the shield and overcutting elements at the back are removed to sustain the shield length of 9m where the lining is activated and initial grout is applied there, (Pang *et al.*, 2005).

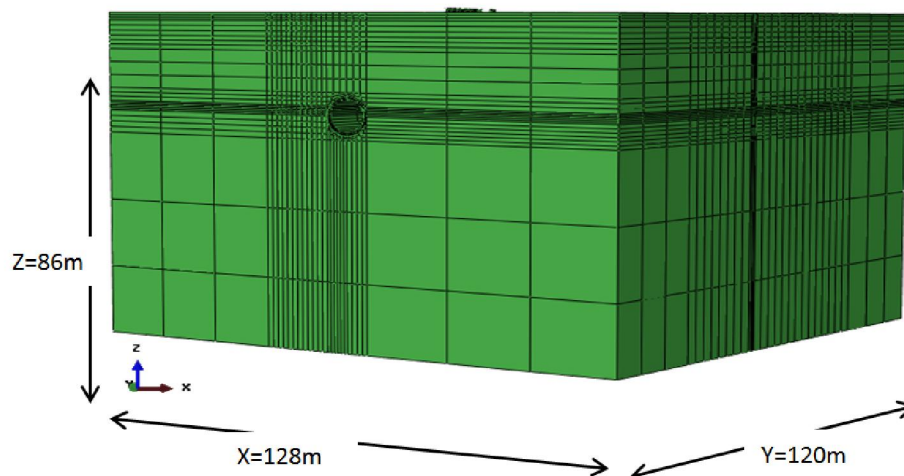


Fig.(7): Finite element mesh used in the Garage El-Attaba case study.

## 2.5 The numerical model results

As mentioned before, the tunnel-ground-piled caps are considered in the numerical modelling of the case study. It must be mentioned that only the four piles caps as discussed in section 2.2 (F1, F2, F3, and F4) are considered in the modelling due the tunnelling insignificant effect on the rest of the pile caps. Fig. (8), shows the surface settlement trough profile at location of measuring elevation reference point (a) during tunnel advancement. On the same figure the distribution of settlement trough profile for the green field conditions (no assignment of the structure) is allocated and the building field settlement compiled during tunnel crossing at point ERP(a), Fig. (2), is defined. The results indicate the propagation of building settlement in accordance to the tunnel advancement. Also, the computed results express relative conformity with building field measurements compiled during construction consequence (at 33 m behind tunnel face & ahead tunnel face by 6 m). The maximum surface settlement trough is recorded when the measuring points is about 18m behind the tunnel face (about 2 times tunnel diameter), and then remained constant. The results also indicate that the mode of the settlement trough profile is absolutely unsymmetrical due to the assignment of the structure in the global

interaction system. It is to be mentioned that the existence of the pile foundations decreases the settlement.

Figures (9&10) illustrate the computed ground surface vertical displacements associated with tunnel advancements at the location of the settlement points SSP.b & SSP.c respectively (figure 2). Comparing the computed surface settlement associated with tunnel advancement with those compiled during tunnel construction, it is obvious that the comparison indicates good signs of agreement between the computed ordinates and the measured values. The results indicate that the ground surface vertical movements at the two points start to take place when the TBM face approaches a distance of about two times tunnel diameter behind the measuring point. During the tunnel advancement the settlement increases in S- shape manner. The maximum rate of settlement occurs when the TBM face moves from a distance 1D behind the surface settlement point to a distance of +1.5D a head of the surface settlement point. After a distance of 1.5 D, the rate of the vertical settlement is decreased before reaching constant deformation condition. In addition, after a distance of 2.5 times tunnel diameter the rate of increase of the value of surficial settlement is almost vanished.

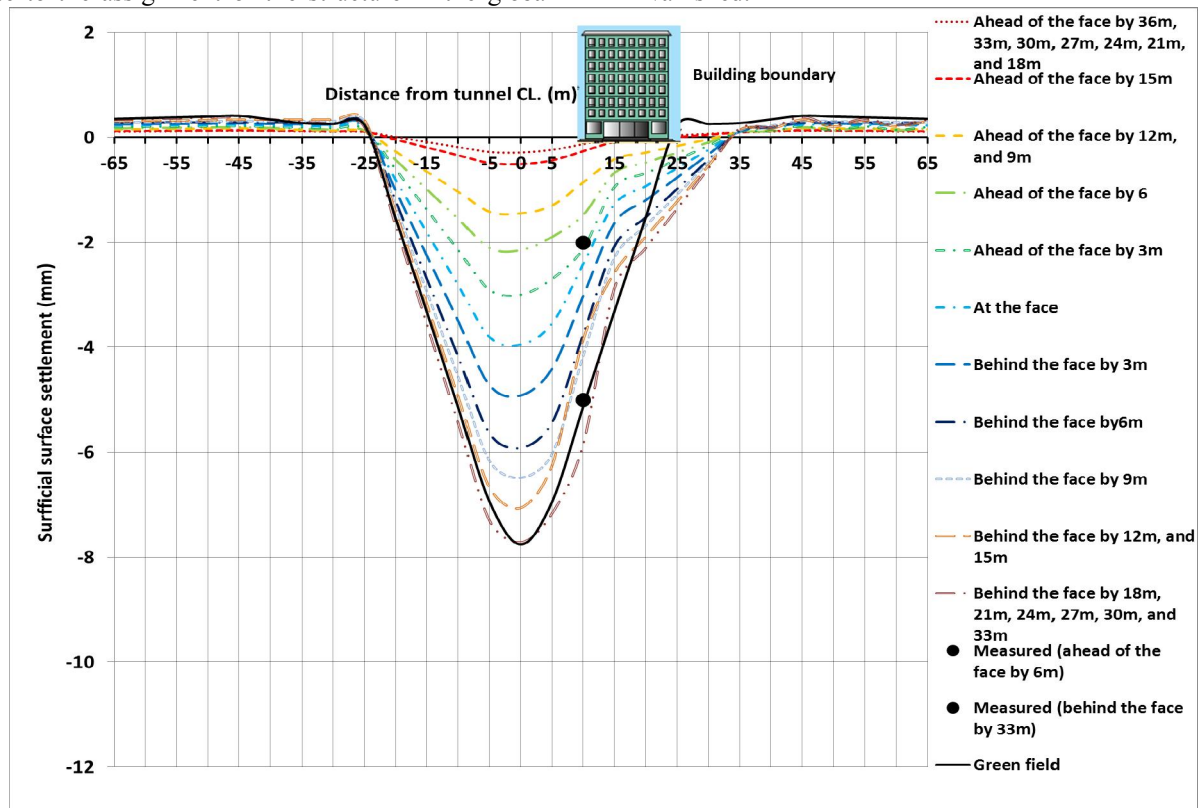


Fig. (8): The computed vertical settlement trough at the location of the elevation reference point (ERP.a) during tunnel advancement

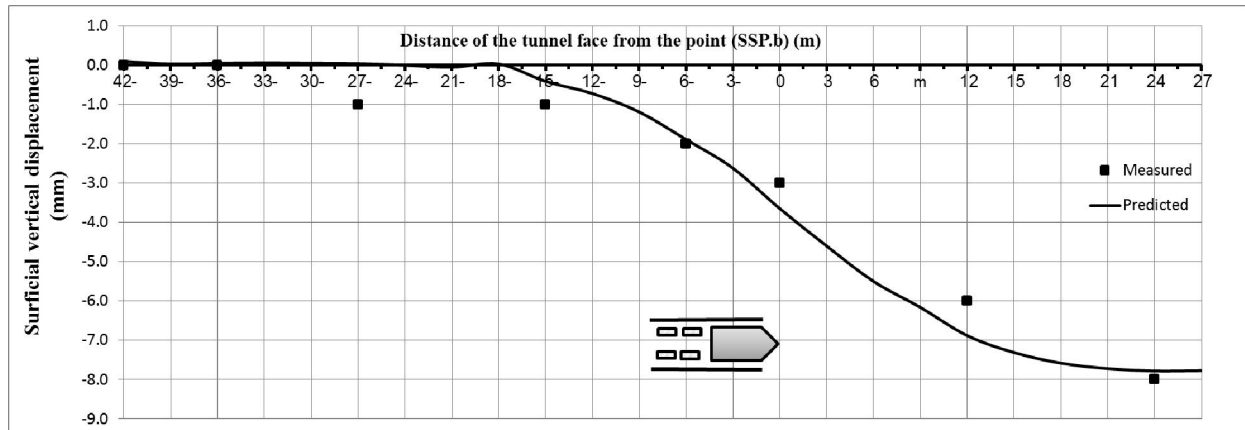


Fig. (9): The computed surficial settlements at point (SSP.b) relative to tunnel advancement.

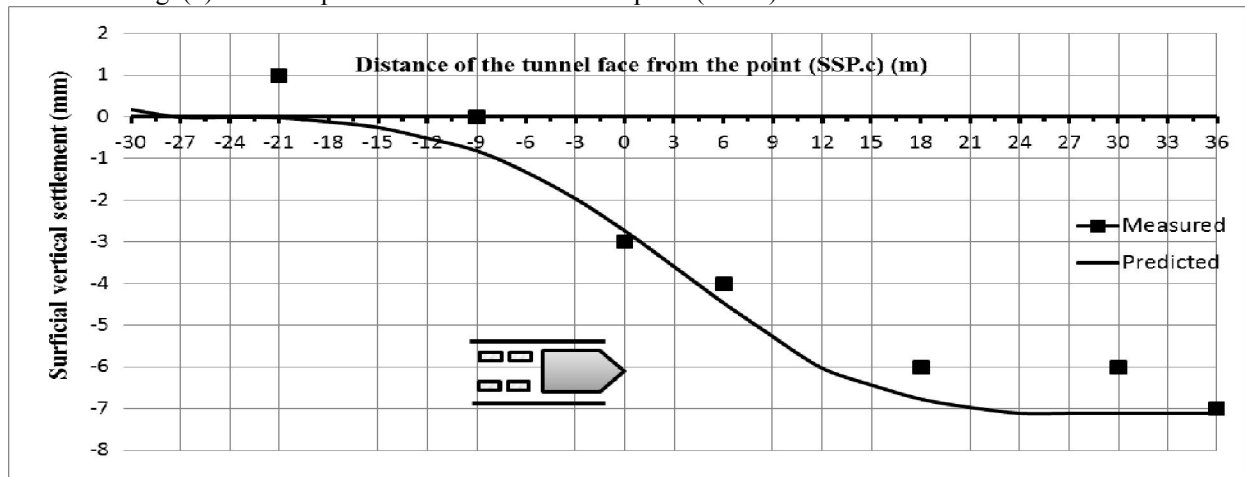


Fig. (10): The computed surficial settlements at point (SSP.c) relative to tunnel advancement

Fig.(11) demonstrates a comparison between the computed vertical movements of the building at the fixed measuring point (a) in association to the tunnel advancement and the measured settlement values

compiled during tunnel crossing. It can be concluded that there is a fairly agreement between the computed and measured settlement point a, b, and c.

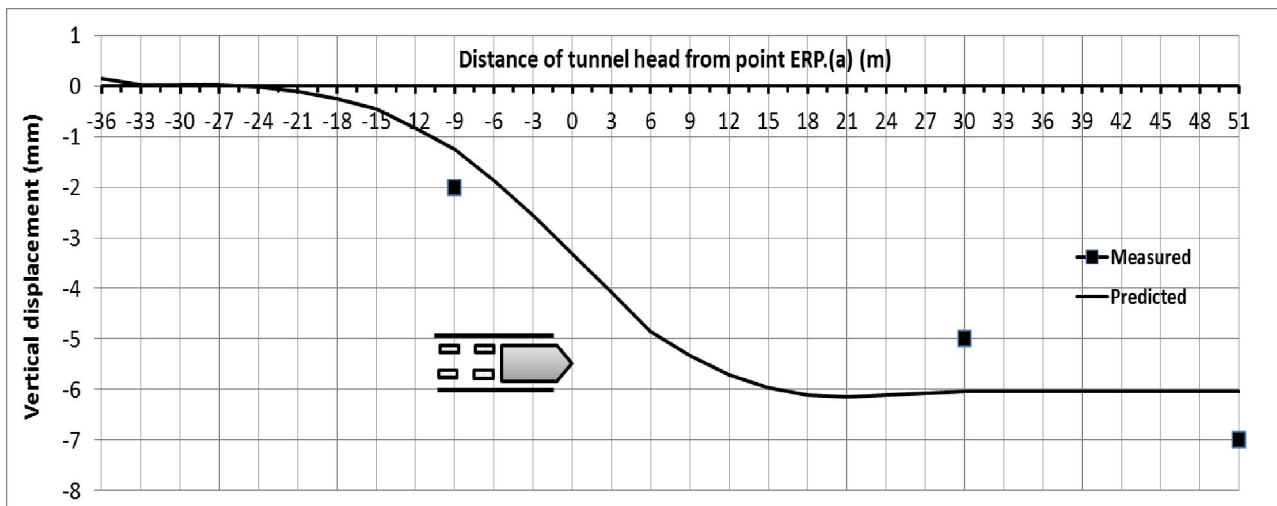


Fig. (11): The computed building settlements at point (a) relative to tunnel advancement.

### 3. Line I project between stations Zirgozar and Zand Crosscase study

The growth of Shiraz City (southern of Iran) managed to assembly of subway in order to overcome the transportation problems. The south eastern part of Line I of that subway with length of approximately 14 km comprised of a twin tunnels. The tunnels were excavated using Earth Pressure Balanced machine (EPB) of 6.88 m external diameter with tail grouting. The tunnel lining is precast reinforced concrete segments forming an internal tunnel diameter of 6 m. A particular interest of Line I project between Stations Zirgozar and Zand Cross was the assemblies of tunnels below an existing Zand Underground

Motorway (Zand Underpass). Fig. (12), demonstrates the longitudinal section of Shiraz tunnel between the stations, under the Zand Underpass. The distance between the stations is 1215 m whereas the underpass length is about 607 m. Next to the Zand Underpass, cars must pass downward and upward ramps of 6.5% with lengths of 135 m. The twin tunnel underneath, on the other hand, were excavated with a generally more gentle slope of 1.9% running from the stations to their deepest point of approximately 16 m along the Underpass. The spacing of the two tunnel centrelines next to the Underpass is equivalent to two tunnel diameters.

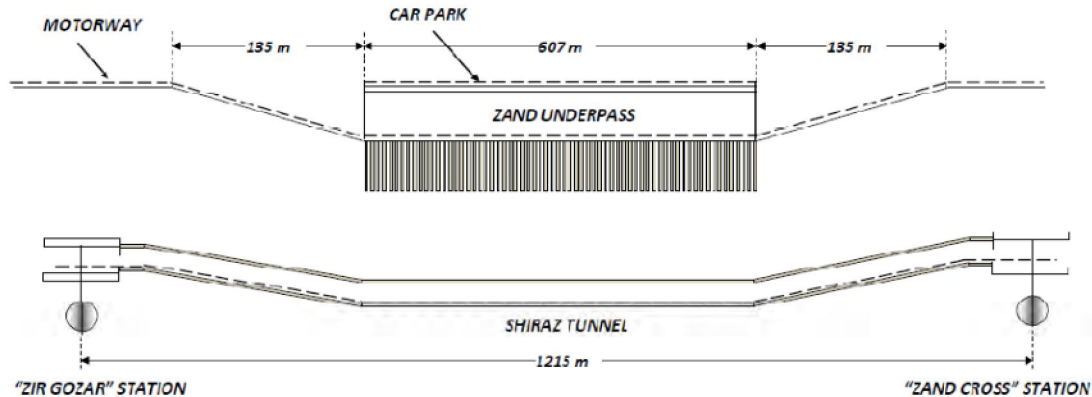


Fig. (12): longitudinal section through the tunnels, (after Namazi, et al., 2011).

#### 3.1 Ground conditions

The geotechnical investigation was carried out in view of the results of three boreholes, (Bamrah Const., 2004). The soil stratifications identified from these boreholes are outlined in Fig., (13). The ground profile started with made ground of about 4 m thick, followed by about 3.2 m depth of clayey sand layer overlying the intermittent layers of clayey sand and inorganic silt, as illustrated in Fig. (13). The tunnels were excavated in the clay and inorganic silt. Table (2) reviews the geotechnical characteristics of the encountered soil strata. The ground watertable was encountered at about 8m below the ground surface.

#### 3.2 Finite element numerical modelling

The finite element idealization utilized to simulate the tunnel-ground-piled walls of the underpass is presented in Fig. (14). The ground continuum, tunnel

lining, gap parameter, tail grouting, shield machine, and piledwalls are modelled using 20-noded continuum solid element. The elastic-plastic soil behaviour is modelled using the Mohr-coulomb failure criterion. The lining and shield machine are idealized as linear elastic material. The elastic properties of the concrete lining and shield are;  $E_{\text{lining}} = 14\text{GPa}$ ,  $\nu_{\text{lining}} = 0.15$ ,  $E_{\text{shield}} = 200\text{GPa}$ , and  $\nu_{\text{shield}} = 0.3$  respectively. The grout elastic properties in the initial liquied state are assigned as;  $E_{\text{grout}} = 750\text{ kPa}$ ,  $\nu_{\text{grout}} = 0.2$ , while the grout elastic moulus reaches 50MPa in the hardening state. Also, piled walls are assigned to behave as linear elastic where,  $E_{\text{pile}} = 19.23\text{ GPa}$ . The slab was modeled as an isotropic elastic solid element with Young's modulus of 23 GPa, poisson's ratio of 0.15, and thickness of 0.8m.

Table (2): Ground strata geotechnical properties (after Bamrah, Const. 2004).

Soil type	$\gamma_b$ (kN/m <sup>3</sup> )	$\gamma_{\text{sat}}$ (kN/m <sup>3</sup> )	E (MPa)	$\nu$	$\phi$	$\Psi$	C (kPa)
Made ground	16	19	51.5	0.3	25°	0	20
Clayey sand	17.7	22.8	88.3	0.25	29°	0	24.5
Inorganic silt	16.9	20.9	30	0.25	36°	0	10

Note:  $\gamma$ = soil density,  $\phi$ = the internal angle of friction, C= soil cohesion, E= Elastic modulus,  $\nu$ = the poisson's ratio,  $\Psi$ = dilation angle



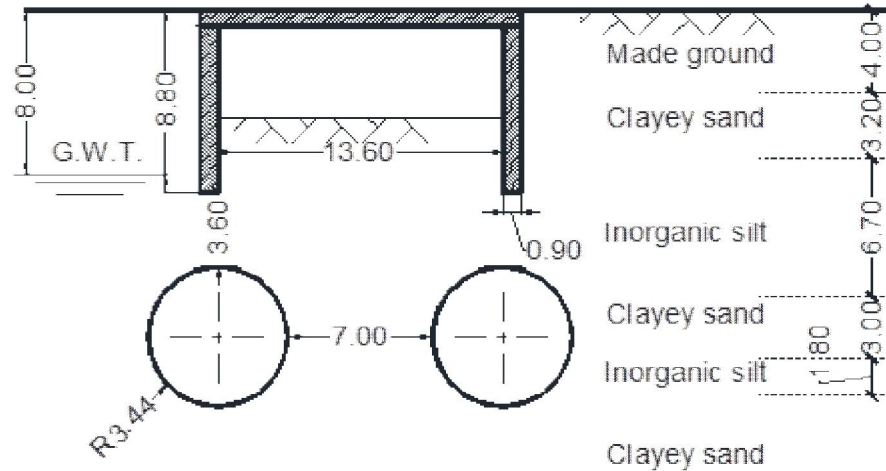


Fig. (13): Description of geotechnical conditions of the site, (after Namazi et al., 2011).

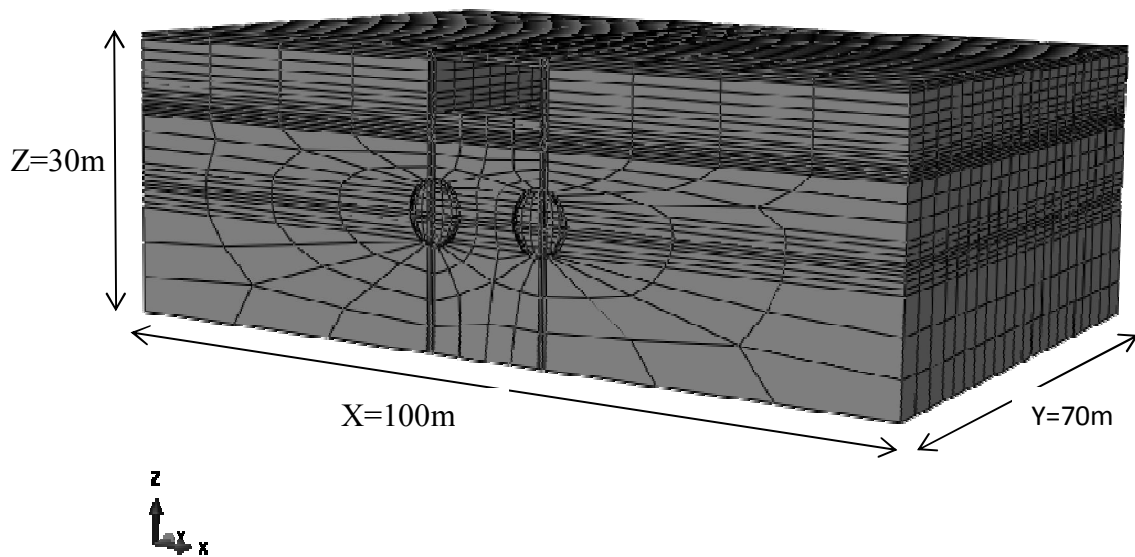


Fig. (14): Finite element mesh used in Shiraz metro case study.

### 3.3 Simulation of tunnelling

Generally, the procedure of tunnel construction was modelled in two stages. The initial insitu conditions before tunnelling, which is achieved by specifying the distribution of effective vertical and horizontal stresses. The initial insitu conditions are fulfilled with simulating the piled walls. The vehicles loads are estimated and applied to the model. The second stage is started after determining the initial conditions and the analyses is continued with the idealization of the first tunnel. The tunnel advancement is idealized on 16 phases. Each phase consists of; (i) deactivation of the excavated soil elements, (ii) activation of shield and overcutting elements, (iii) applying face pressure on the face elements, (iv) introducing of the tunnel lining elements, and (v) activate the time-dependent setting

grouting elements (overcutting elements) of the gap between the soil and the newly installed lining. The excavation phase length is 3m-length.

Then, the second tunnel is idealized after setting up the final field of the ground movements associated with the construction of the first tunnel. The analyses of the second tunnel are subsequently takes place following the same computation procedure, and the final integrated filed of the ground deformations associated with construction of the twin tunnels are achieved.

### 3.4 Numerical modelling results

The results of the final computed ground surface settlements around the underpass walls, the surface movement of the bottom slab, and the vertical displacements of the two piled walls are illustrated in Fig. (15). Correspondingly, the green filed ground

deformation (no assignment of the underpass) and the compiled field deformations during construction phase are also illustrated on Fig. (15). While, the settlement trough associated with construction of first tunnel only is outlined in Fig. (16). The figures indicate that the ordinates of ground vertical displacements associated with tunnelling are greater than those computed for the green field conditions, which attributed to the existence of the underpass piled walls directly in the zones characterized with maximum ground movements towards the tunnel to fill the gap due shield overcutting.

Comparing the final computed results of the ground and the wall displacements with the measured displacements indicate good signs of agreement. Fig.(17) illustrates a comparison between the settlement trough profiles at the ground surface and at the piled walls base level. The figure indicates that the surface settlement trough profile is wider than that induced at pile base. However, it is clear that there is no significant difference between the values of settlements above two tunnels (I) and (II).

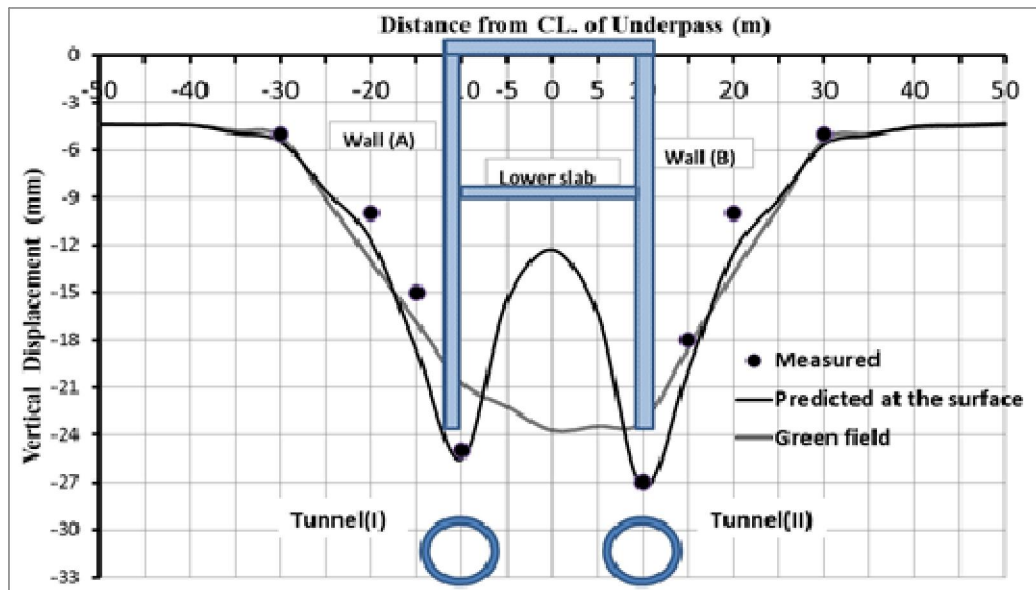


Fig. (15): The final computed ground movements after tunnels construction.

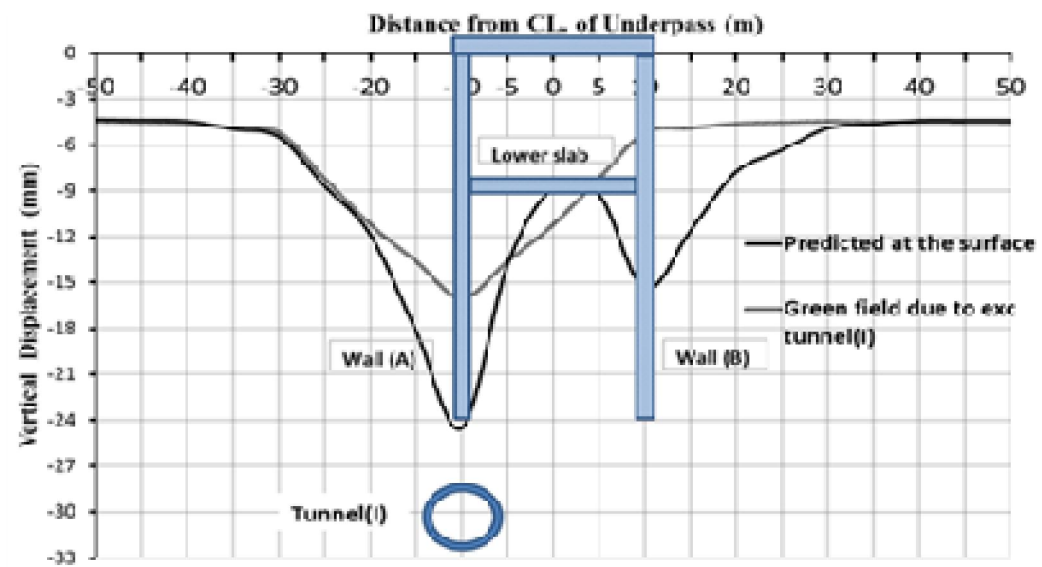


Fig. (16): The final computed ground movements after the construction of tunnel (I).

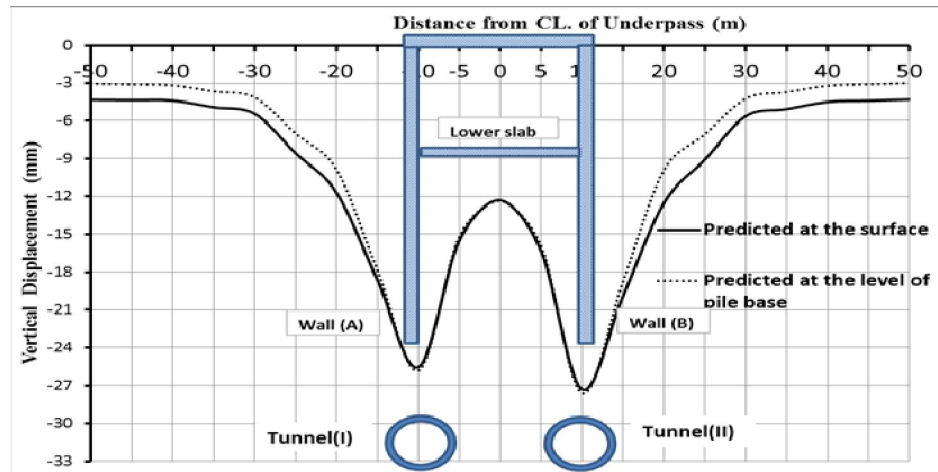


Fig. (17): Settlement trough profiles at in accordance of tunnel advance.

#### 4. Conclusion

Two case studies of large tunnel projects constructed closer or nearby piled foundation systems are idealized in the analysis of three dimensional numerical modelling of ground-tunnelling-piles interaction. Comparing the computed results with the field measurements compiled during the construction of both projects indicated the capability of the proposed numerical model to update the ground deformations associated with tunnelling. The results indicated that modelling such complicated interaction features is a typical three-dimensional problem in which the details of the tunnelling activities must be introduced through the modelling, as well as the simulation of tail skin grouting setting. Also, the idealization of the piling systems in the details of the three-dimensional modelling is very essential to update a more realistic idealization for such complicated geotechnical problems. Also, the present study ensured the need for back analysis procedure to update or modifying the design approaches of similar geotechnical problems.

#### References:

1. Bamrah Construction. (2004). "Geotechnical engineering of Shiraz subway report". Shiraz Subway Construction Company, Shiraz, Iran (In Persian).
2. Burland J B, Standing J R and Jardine F M (2002). "Building response to tunnelling". Case studies from construction of the Jubilee Line Extension, London. Thomas Telford, London.
3. Cheng, C.Y., Dasari, G.R., Leung C.F., Chow, Y.K. and Rosser, H.B. (2004). "3D Numerical Study of Tunnel-Soil-Pile Interaction", Proceedings of World Tunnel Congress and 13th ITA Assembly, Singapore.
4. Pang, C.H., Yong, K.Y., and Chow, Y.K. (2005). "Three-dimensional numerical simulation of tunnel advancement on adjacent pile foundation", Analysis of the Past and Lessons for the Future – Erdem & Solak (eds), National University of Singapore, Singapore, ISBN 04 1537 452 9.
5. Hamza Associates, (2002). "Geotechnical investigation report: Greater Cairo Metro-Line 3".
6. Hibbitt, Karlsson & Sorensen, Inc (2003). ABAQUS User's manual, Version 6.11.
7. Loganathan, N., Poulos, H. G. and Xu, K. J. (2001). "Ground and pile-group response due to tunnelling". Soils and Foundations, Vol. 41, No. 1, pp. 57-67.
8. Mindess, S., & Young, J., F., (1981), Concrete, Englewood Cliffs, N.J., Prentice Hall.
9. McCarthy Brothers company, (1984). A division of design and management, consultant of Ataba Parking Garage, Cairo, Egypt.
10. Mroueh, H. and Shahrour, I. (2002). "Three-dimensional finite element analysis of the interaction between tunnelling and pile foundations". Int. Journal for Numerical and Analytical Methods in Geomechanics, Vol. 26, pp. 217-230.
11. National Authority for Tunnels (NAT), (2009), Project Document.
12. National Authority for tunnel, (2010). "Tunnel from Attaba to Geish shaft monitoring measurements", contract N° 49/Metro, phase 1", Greater Cairo Metro, pp.270-271.
13. Namazi, E, Mohamad, H, Jorat, M,E, and Hajihassani, M, (2011). "Investigation on the Effects of Twin Tunnel Excavations Beneath a Road Underpass", J.of EJGE, Vol. 16, pp.441-450.
14. Shirlaw, J.N., Richards, D.P., Ramond, P. and Longchamp, P., (2004). "Recent experience in automatic tail void grouting with soft ground tunnel boring machines", ITA-AITES, World Tunnel Congress, pp. 22-27, May 2004, Singapore.